Hyperlipidemia is necessary for the initiation and progression of atherosclerosis by severe periodontitis in mice

JIN SOOK SUH[1*], SHARON Y.J. KIM[1*], SUNG HEE LEE[1], REUBEN H. KIM[1,2] and NO-HEE PARK[1-3]

[1]The Shapiro Family Laboratory of Viral Oncology and Aging Research, School of Dentistry; [2]UCLA Jonsson Comprehensive Cancer Center; [3]Department of Medicine, David Geffen School of Medicine, University of California, Los Angeles, CA 90095, USA

Received February 24, 2022; Accepted June 7, 2022

DOI: 10.3892/mmr.2022.12789

Abstract. Hyperlipidemia is a major risk of atherosclerosis; however, systemic inflammatory diseases such as rheumatoid arthritis, psoriasis, systemic lupus erythematosus and systemic sclerosis are also known risks for the development of atherosclerosis. Periodontitis, a local and systemic inflammatory condition, has also been reported as a risk for atherosclerosis, but the specific link between periodontitis and atherosclerosis remains somewhat controversial. We previously reported that ligature-induced periodontitis exacerbates atherosclerosis in hyperlipidemic Apolipoprotein E-deficient (*ApoE*$^{-/-}$) mice. To understand whether hyperlipidemia is necessary for the development and exacerbation of atherosclerosis associated with periodontitis, the present study created ligature-induced periodontitis in both wild-type (WT) and *ApoE*$^{-/-}$ mice. Subsequently, the status of local, systemic and vascular inflammation, serum lipid contents and arterial lipid deposition were examined with histological analysis, μCT, *en face* analysis, serum lipid and cytokine measurements, reverse transcription-quantitative PCR and immunohistochemical analysis. Ligature placement induced severe periodontitis in both WT and *ApoE*$^{-/-}$ mice at the local level as demonstrated by gingival inflammation, alveolar bone loss, increased osteoclastic activities and inflammation in alveolar bone. Systemic inflammation was also induced by ligature placement in both WT and *ApoE*$^{-/-}$ mice, albeit more so in *ApoE*$^{-/-}$ mice. The serum cholesterol levels were not altered by the ligature in both WT and *ApoE*$^{-/-}$ mice. However, the vascular inflammation and arterial lipid deposition were induced by ligature-induced periodontitis only in *ApoE*$^{-/-}$ mice, but not in WT mice. The present study indicated that the coupling of systemic inflammation and hyperlipidemia was necessary for the development and exacerbation of atherosclerosis induced by ligature-induced periodontitis in mice.

Correspondence to: Dr No-Hee Park or Dr Reuben H. Kim, The Shapiro Family Laboratory of Viral Oncology and Aging Research, School of Dentistry, University of California, 10833 Le Conte Avenue, Los Angeles, CA 90095, USA
E-mail: nhpark@g.ucla.edu
E-mail: rkim@dentistry.ucla.edu

*Contributed equally

Key words: atherosclerosis, hyperlipidemias, periodontitis, systemic inflammation

Introduction

Periodontitis is a chronic oral inflammatory response of the periodontium that affects almost 50% of US adults ≥30 years of age (1,2). This chronic, multifactorial disease is characterized by gingival inflammation and alveolar bone loss (3). Periodontitis can trigger an immune-inflammatory response that ultimately leads to a non-reversible change of bone supporting tissues, resulting in progressive destruction of alveolar bone and finally tooth loss (4). Periodontitis has also been reported to be associated with the development of several systemic diseases, such as rheumatoid arthritis, psoriasis, systemic sclerosis, Alzheimer's disease and cardiovascular diseases (CVD) (5). Among the systemic diseases associated with periodontitis, CVD has received the most attention, as a number of epidemiological and clinical studies have indicated a strong association between periodontitis and CVD (6,7). Periodontitis clearly imparts adverse risks for CVD in clinical evidence in addition to animal models (8,9).

Atherosclerosis is a degenerative vascular disease accompanying chronic and progressive vascular inflammatory conditions, which results in fatal consequences such as myocardial infarction and stroke due to the development of atherosclerotic plaque (10). Although hyperlipidemia is known as a major risk factor for the development of atherosclerosis, previous studies have indicated that systemic inflammation plays a notable role in the initiation and progression of atherosclerosis and is also one of the precipitating factors for atherogenesis (11,12). Systemic inflammation (such as increased serum proinflammatory cytokine levels) is known to induce vascular inflammation, resulting in vascular endothelial cell dysfunction, an early important step of atherogenesis. Also, vascular inflammation causes atheroma progression and complications by inducing the proliferation and migration of vascular smooth muscle cells, resulting in thrombosis (13).

There are several systemic inflammatory diseases that are known to increase the risk of atherosclerosis development, such as rheumatoid arthritis, psoriasis, systemic lupus

erythematosus (SLE) and systemic sclerosis (14). Periodontitis, a local and systemic condition, has also been suggested to be one of the putative risk factors for atherogenesis (15-18). We previously reported that ligature-induced periodontitis induces severe systemic inflammation and exacerbates atherosclerosis in hyperlipidemic Apolipoprotein E-deficient (*ApoE*$^{-/-}$) mice (19); however, to the best of our knowledge, the effect of severe periodontitis on atherogenesis in normolipidemic condition remains unknown. To understand whether hyperlipidemic condition is necessary for the development and exacerbation of atherosclerosis associated with periodontitis, the present study investigated the effect of ligature-induced periodontitis on atherogenesis in normolipidemic wild-type (WT) and hyperlipidemic *ApoE*$^{-/-}$ mice.

Materials and methods

Animals. A total of 20 male WT and *ApoE*$^{-/-}$ C57BL/6 mice (Jackson Laboratory) that were 7 weeks old (mean weight, 19 g), were housed in the vivarium at The University of California (Division of Laboratory Animal Medicine, Los Angeles, USA). All mice were housed in a pathogen-free animal experimental facility of University of California, Los Angeles, under a 12 h light/dark cycle at 20˚C, with 40% humidity, and proper ventilation and air circulation. The mice were fed with a high-fat diet (HFD) for 14 weeks (cat. no. D12079B; Research Diets, Inc.) to facilitate the development of atherosclerosis (19). All mice had free access to the food and drinking water. Mice health and behavior were monitored every other day throughout the whole duration of the experiment (14 weeks). No mice were found dead during the experimental period. Isoflurane (99.9%) and a mixture of ketamine (100 mg/kg) and xylazine (5 mg/kg) were used as anesthetics during ligature placement. Carprofen (3 mg/kg), a pain relief drug, was also used once a day for 3 days after ligature placement to minimize pain of the mice. All mice were euthanized under general anesthesia using isoflurane (99.9%) to minimize suffering. Euthanasia was performed via cardiac perfusion, and the heartbeats of the mice were assessed for 5 min to verify death. All experiments were approved by the Chancellor's Animal Research Committee of the University of California, Los Angeles (approval no. ARC # 2019-057-01A).

Induction of periodontitis in mice. At 1 week after starting the HFD, the mice were divided into four groups (five mice per group) as follows: i) WT control mice (WT/no lig.); ii) ligature-placed WT mice (WT/with lig.); iii) *ApoE*$^{-/-}$ mice (*ApoE*$^{-/-}$/no lig.); and iv) ligature-placed *ApoE*$^{-/-}$ mice (*ApoE*$^{-/-}$/with lig.). The 6-0 silk ligature (MilliporeSigma) was placed around the second molars under general anesthesia using Ketamine/Xylazine (100 and 5 mg per kg, respectively) via intraperitoneal injection as described previously (20).

Tissue collection and histological analysis. Whole blood was collected from mice by cardiac puncture under general anesthesia with isoflurane (Abbott Laboratories). The mice were then perfused and fixed with 4% paraformaldehyde at room temperature in phosphate-buffered saline (PBS) via the left ventricle for 5 min. After the perfusion, the heart, the carotid artery and the full-length of the aorta-to-iliac bifurcation were exposed and dissected carefully from any surrounding tissues. The heart and artery samples were embedded in Scigen Tissue-Plus O.C.T. Compound (Thermo Fisher Scientific, Inc.), and sectioned at 7-μm thickness. A total of 12 sections at 100 μm intervals were collected from each mouse and stained with Oil red O (Sigma-Aldrich; Merck KGaA) at room temperature for 15 min to quantify atherosclerotic burden at the sinus lesion. The maxillae were excised and half of the palatal tissues were harvested using a blade for gene expression analysis. For micro-computed tomography (μCT) analysis, the maxillae were fixed with 4% paraformaldehyde in PBS, pH 7.4, at 4˚C overnight and stored in 70% ethanol solution at 4˚C.

After μCT scanning, the maxillae were decalcified using 5% EDTA and 4% sucrose in PBS (pH 7.4) for 3 weeks at 4˚C. The decalcification solution was changed daily. Decalcified maxillae were processed for paraffin embedding blocks at the UCLA Translational Procurement Core Laboratory. Blocks were sectioned at 5-μm intervals using a microtome (Thermo Fisher Scientific, Inc.). The sections were dewaxed at 60˚C for 30 min, and were then rehydrated at room temperature by incubating the sections twice in xylene for 5 min, twice in 100% ethanol for 2 min, twice in 95% ethanol for 2 min and in 70% ethanol for 2 min. After the sections were rinsed with running tap water for 1 min at room temperature, the sections were stained with hematoxylin and eosin for 30 min at room temperature (Sigma-Aldrich; Merck KGaA). For tartrate-resistant acid phosphatase staining, the sections were stained using an acid phosphatase kit (cat. no. 378A; Sigma-Aldrich; Merck KGaA), according to the manufacturer's protocol, and then counterstained using hematoxylin for 20 min at room temperature. The digital images of the stained sections were obtained using the DP72 light microscope (Olympus Corporation). The clinical attachment loss was observed under the microscope by measuring cement-enamel junction (CEJ) to the base of the pocket depth by an investigator (JS). The reading was confirmed in a double blind manner by another individual (N-HP).

μCT and histological analysis of maxillae. The fixed maxillae were subjected to μCT scanning (Skyscan1275; Bruker Corporation) using a voxel size of 20 μm^3 and a 0.5 mm aluminum filter at 55 kVp and 145 μA. Two-dimensional slices from each maxilla were combined using NRecon and CTAn/CTVol programs (Bruker Corporation) to form a three-dimensional reconstruction. Alveolar bone loss was quantified by measuring the distance from the palatal and mesiobuccal CEJ to the alveolar bone crest (ABC) of the second molars by an investigator (JS). The reading was confirmed in a double blind manner by another individual (N-HP).

En face analysis. The full-length of the aorta-to-iliac bifurcation was opened along the ventral midline and dissected free of the animal under a stereomicroscope (Stemi 305; Zeiss AG). For *en face* analysis, the aorta was stained with Sudan IV (Sigma-Aldrich; Merck KGaA) as previously described (9) and pinned out flat, intimal side up, between cover slides. Aortic images were captured using a Nikon digital camera (Nikon Corporation) and the intensity of lipid

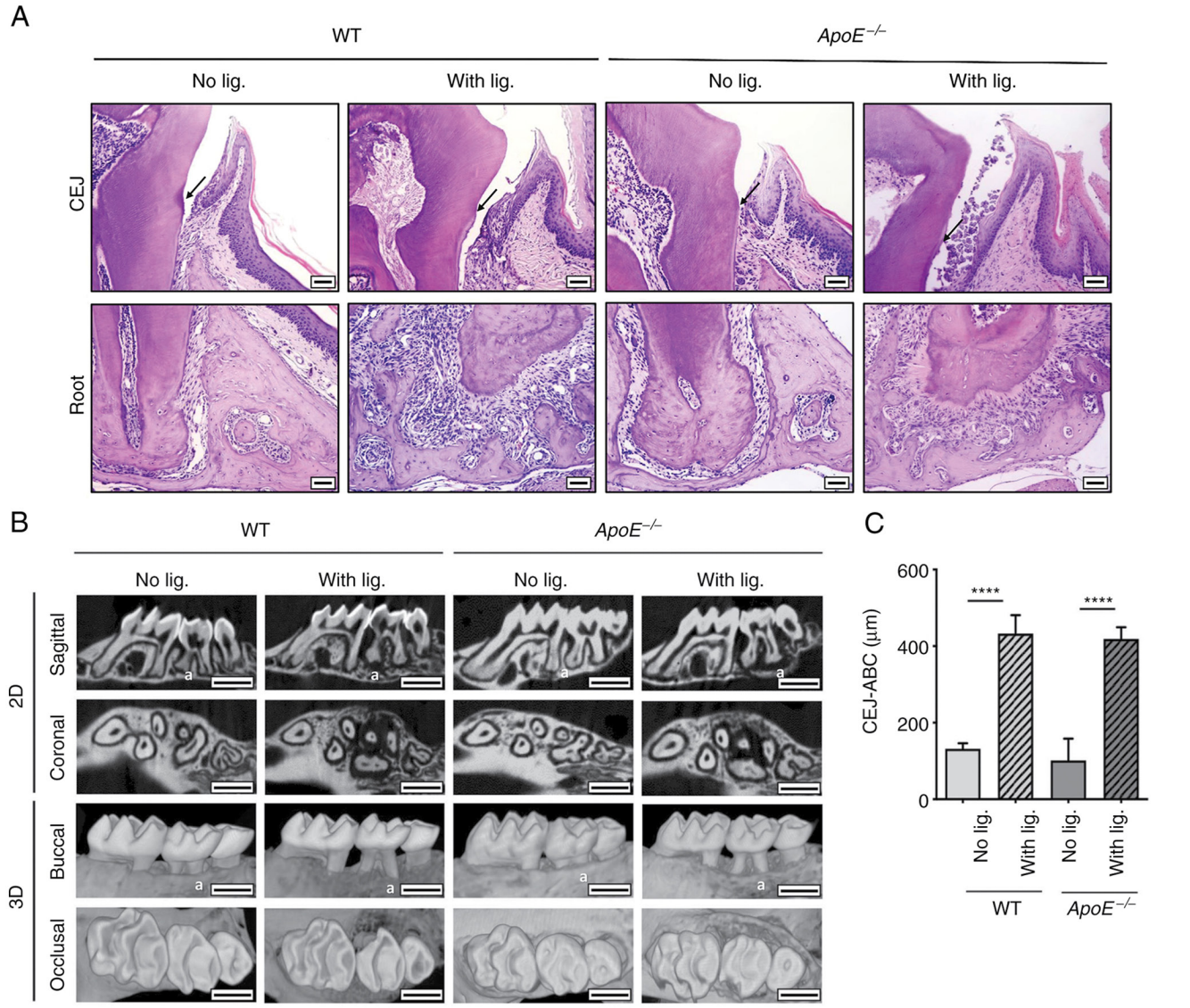

Figure 1. Evaluation of periodontitis induced by ligature placement in WT and *ApoE*$^{-/-}$ mice fed with HFD. (A) Hematoxylin and eosin staining on the periodontium of maxillary second molar (scale bar, 50 μm). Black arrows indicate the CEJ. There was notable epithelial detachment around the molars of mice receiving ligature placement. (B) Representative 2D or 3D μCT images of mouse maxilla (scale bar, 1 mm). a, alveolar bone. There was severe alveolar bone loss around the second molars of mice receiving ligature placement. (C) Alveolar bone loss measured at the distobuccal and palatal roots of the maxillary second molars from CEJ to ABC. ****P<0.0001. CEJ, cement-enamel junction; ABC, alveolar bone crest; WT, wild-type; *ApoE*$^{-/-}$, Apolipoprotein E-deficient; HFD, high-fat diet.

staining was analyzed using ImageJ software version 1.48 (National Institutes of Health).

Serum lipid and cytokine measurements. Levels of total cholesterol (TC), triglycerides (TG), high density lipoprotein (HDL) and low-density lipoprotein (LDL) were measured using a Cholesterol Assay kit (Abcam) in the UCLA Cardiovascular Core Facility (21). The serum levels of TNF-α, IL-1β and IL-6 were measured by ELISA using Ready-SET-go kits [TNF-α Mouse Uncoated ELISA kit with Plates (cat. no. 88732422); IL-6 Mouse Uncoated ELISA Kit with Plates (cat. no. 88706422); IL-1β Mouse Uncoated ELISA kit with Plates (cat. no. 88701322); Thermo Fisher Scientific, Inc.] according to the manufacturer's protocol. The color reaction was stopped with the addition of Stop solution (BioLegend, Inc.), and absorbance was read immediately using a plate reader at 450 nm (Bio-Rad Laboratories, Inc.). The standard curve was calculated by plotting the standards against the absorbance values, and the cytokine levels were measured in pg/ml.

Reverse transcription-quantitative PCR (RT-qPCR). Total RNA from mouse tissues was extracted using RNeasy micro kit (cat. no. 74106; Qiagen GmbH) and reverse-transcribed with the following cycle: 5 min at 65˚C, 2 min at 25˚C and 50 min at 45˚C using SuperScript® III Reverse Transcriptase Synthesis kit (cat. no. 18064014; Thermo Fisher Scientific, Inc.). Subsequently, qPCR was performed under the following conditions: Pre-incubation at 95˚C for 2 min; amplification at 95˚C for 15 sec, 57˚C for 15 sec and 72˚C for 1 min, for 55 cycles; melting curve at 95˚C for 15 sec, 60˚C for 1 min and 95˚C for 15 sec using PowerUp™ SYBR Green Master Mix

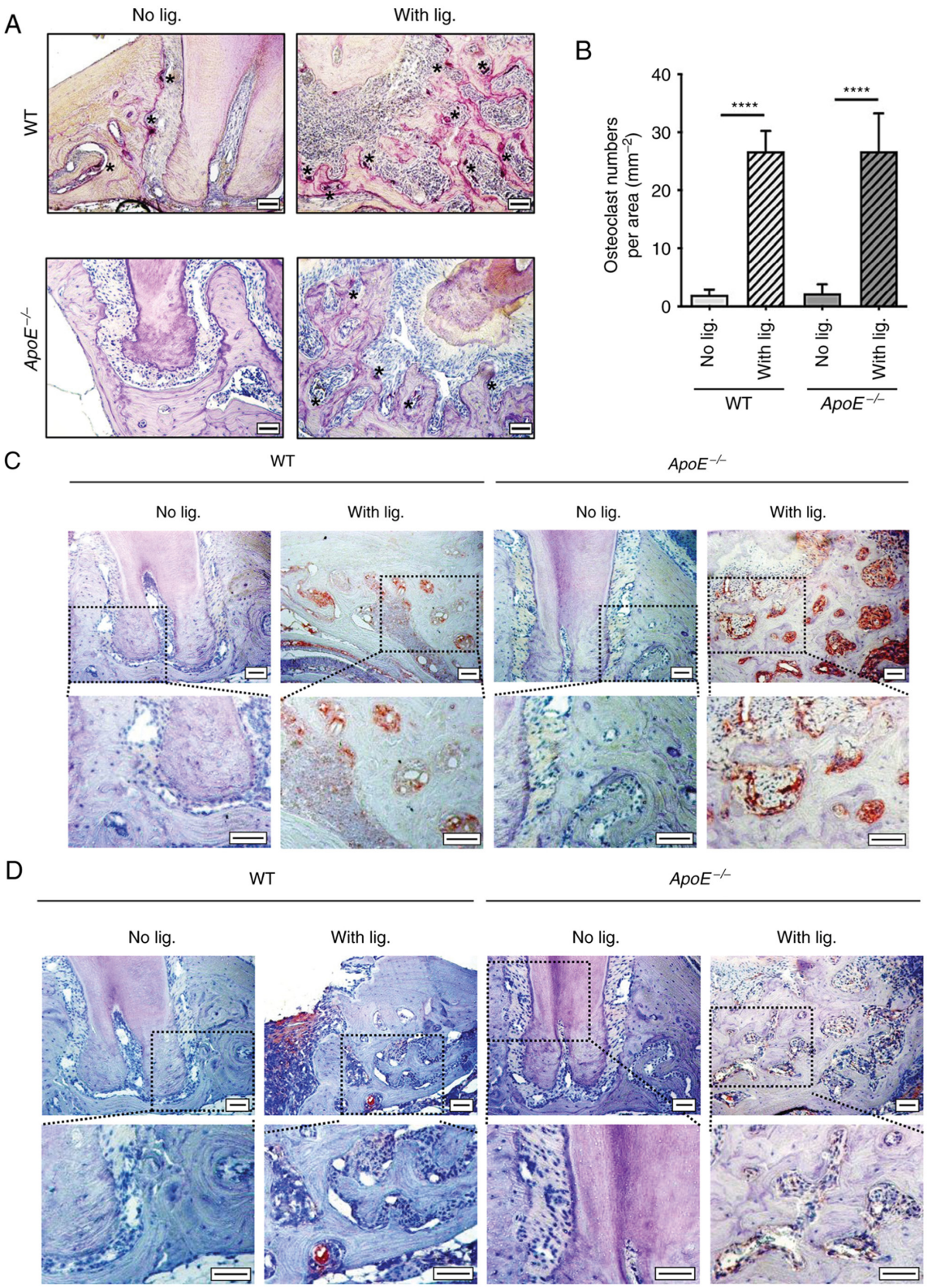

Figure 2. Evaluation of osteoclasts and immunohistochemistry on maxillary tissues placed ligature in WT and *ApoE*$^{-/-}$ mice fed with HFD. (A) TRAP-stained tissues at the maxillary second molar areas. Black stars indicate osteoclasts. Scale bar, 50 μm. (B) Average number of TRAP+ osteoclasts per mm2 of alveolar bone. ****P<0.0001. Immunohistochemistry of (C) CD68 antibody and (D) p65 antibody on the periodontium of maxillary second molar. Scale bar, 50 μm. TRAP, Tartrate-resistant acid phosphatase; WT, wild-type; *ApoE*$^{-/-}$, Apolipoprotein E-deficient; HFD, high-fat diet.

(cat. no. A25741; Thermo Fisher Scientific, Inc.) according to the manufacturer's protocol. The following primers were used for qPCR: TNF-α forward, 5'-TCAGGTTGCCTCTGTCTCAG-3', and reverse, 5'-GCTCTGTGAGGAAGGCTG TG-3'; *IL-1β* forward, 5'-CACAGCAGCACATCAACA AG-3', and reverse, 5'-GTGCTCATGTCCTCATCCTG-3'; *IL-6* forward, 5'-TGGGACTGATGCTGGTGACA-3', and reverse 5'-GCCTCCGACTTGTGAAGTGGT-3'; and *β-actin*

forward, 5'-CATTGCTGACAGGATGCAGAAGG-3', and reverse 5'-TGCTGGAAGGTGGACAGTGAGG-3'. *β-actin* served as control and the fold induction was calculated using the comparative ΔCq method (22). Data were presented as relative transcript levels ($2^{-\Delta\Delta Cq}$).

Immunohistochemical (IHC) staining. The slides containing the maxilla sections were submerged in a citric acid-based antigen unmasking solution (Vector Laboratories) at 65˚C overnight for antigen retrieval and then incubated with anti-CD68 antibody (cat. no. ab125212; Abcam) or p65 (cat. no. ab32536; Abcam) as primary antibodies. The tissue sections were visualized using 3-amino-9-ethylcarbazole (AEC; cat. no. SK-4205; Vector Laboratories, Inc.) at room temperature for 1 min, followed by counterstaining with hematoxylin for 1 min at room temperature, then sealed with ImmunoHistoMount™ solution (Agilent Technologies, Inc.). The digital images of the stained sections were obtained using the DP72 light microscope (Olympus Corporation).

Statistical analysis. All graphs were created and statistical analyses were calculated using GraphPad Prism 9.3.1 (GraphPad Software, Inc.), and for multiple comparisons, one-way ANOVA with Tukey's post hoc test was used. P<0.05 was considered to indicate a statistically significant difference. All *in vitro* results were confirmed by at least three independent experiments. Error bars represent mean ± SEM.

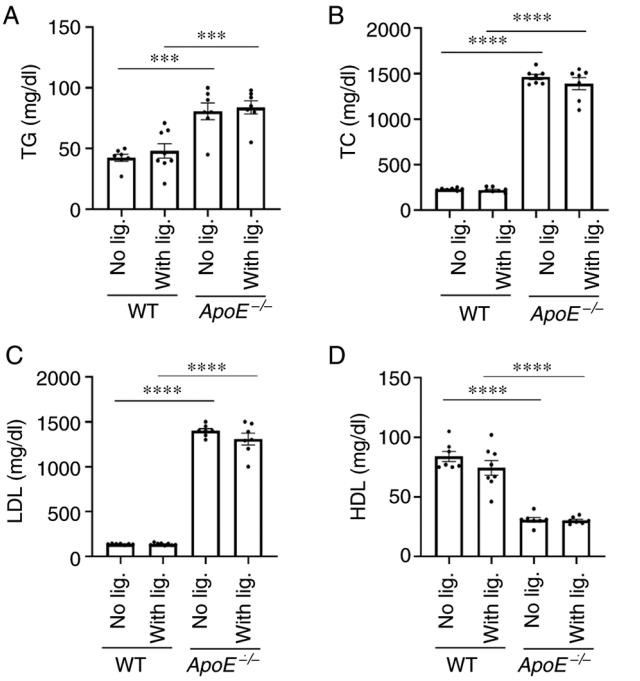

Figure 3. Cholesterol levels in WT and ApoE$^{-/-}$ mice fed with HFD. Mice sera were used and analyzed using ELISA for (A) TG, (B) TC, (C) LDL and (D) HDL. Results represent the means ± SEM from 5 different samples. ***P<0.001, ****P<0.0001. WT, wild-type; *ApoE*$^{-/-}$, Apolipoprotein E-deficient; TC, total cholesterol; LDL, low density lipoprotein cholesterol; HDL, high-density lipoprotein cholesterol; TG, triglyceride.

Results

Development of periodontitis is induced by the ligature placement in WT and ApoE$^{-/-}$ mice. To investigate the effect of periodontitis on atherogenesis in both normolipidemic and hyperlipidemic conditions, periodontitis was induced in WT and *ApoE*$^{-/-}$ mice by placing ligature for 14 weeks as described previously (19). Histological examination revealed that the ligature placement induced alterations in the organization of the junctional epithelium and deep subgingival pockets, such as clinical epithelial attachment loss (Fig. 1A) and alveolar bone loss (Fig. 1B) in both WT and *ApoE*$^{-/-}$ mice compared with the control mice without ligature placement. The μCT analysis revealed a similar alveolar bone loss in both WT and *ApoE*$^{-/-}$ mice with ligature compared with the control mice, as measured by the distance between the CEJ and the ABC (Fig. 1B and C). These data indicate that long-term ligature placement induced a similar degree of periodontitis in both groups of mice.

As local inflammation of periodontium induces alveolar bone loss (23), the presence of osteoclasts, macrophages and inflammation-specific markers, such as p65, were evaluated to examine the status of local inflammation in both WT and *ApoE*$^{-/-}$ mice. Ligature placement significantly increased the numbers of osteoclasts around the ligated tooth in both WT and *ApoE*$^{-/-}$ mice experimental groups, but not in the non-ligated groups (Fig. 2A and B). Furthermore, IHC staining of CD68, a macrophage surface marker, revealed that ligature placement similarly increased the recruitment of macrophages in both WT and *ApoE*$^{-/-}$ mice (Fig. 2C). Ligature placement also upregulated the expression of p65, a subunit of the major inflammatory transcriptional factor, NF-κB (24) in the alveolar bone of both WT and *ApoE*$^{-/-}$ mice (Fig. 2D). These data indicated that ligature placement induced similar degree of periodontitis and local inflammation in both WT and *ApoE*$^{-/-}$ mice.

Differential systemic status of lipid and systemic inflammation in WT and ApoE$^{-/-}$ mice by ligature placement. To determine whether the ligature placement altered lipid content in the blood stream, enzymatic assays were performed to detect the levels of several types of lipids. As expected, the control *ApoE*$^{-/-}$ mice without ligature placement had significantly higher levels of TG, TC and LDL levels in the serum compared with WT control mice, although WT control mice revealed significantly higher HDL levels compared with the *ApoE*$^{-/-}$ control mice (Fig. 3A-D). Notably, the long-term ligature placement did not alter the lipid profiles in both experimental WT and *ApoE*$^{-/-}$ mice when compared with those of control mice without ligature placement (Fig. 3). By contrast, ligature placement significantly increased the serum levels of proinflammatory cytokines, such as, IL-1β, IL-6 and TNFα in the serum of both WT and *ApoE*$^{-/-}$ mice compared in the mice that did not receive ligature placement, although the cytokine levels were markedly higher in *ApoE*$^{-/-}$ mice compared with WT mice (Fig. 4). These data indicated that ligature-induced periodontitis induced systemic inflammation in both WT and *ApoE*$^{-/-}$ mice without altering lipid profiles.

Ligature induced periodontitis enhances arterial lipid deposition and vascular inflammation in ApoE$^{-/-}$ mice, not in WT mice. To examine the atherosclerosis development,

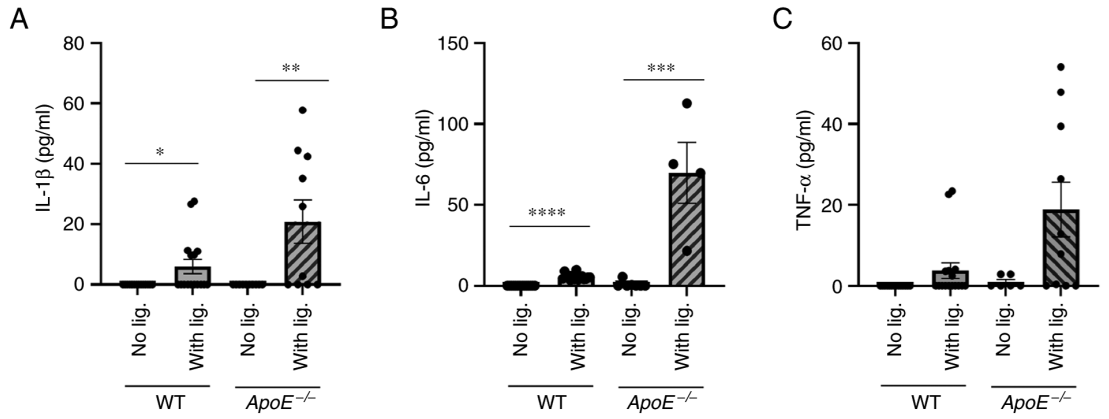

Figure 4. Levels of pro-inflammatory cytokines in WT and *ApoE*$^{-/-}$ mice fed with HFD. Mice sera was analyzed using ELISA for (A) IL-1β, (B) IL-6 and (C) TNF-α. Results represent the means ± SEM from 5 different samples. *P<0.05, **P<0.01, ***P<0.001, ****P<0.0001. WT, wild-type; *ApoE*$^{-/-}$, Apolipoprotein E-deficient; HFD, high-fat diet.

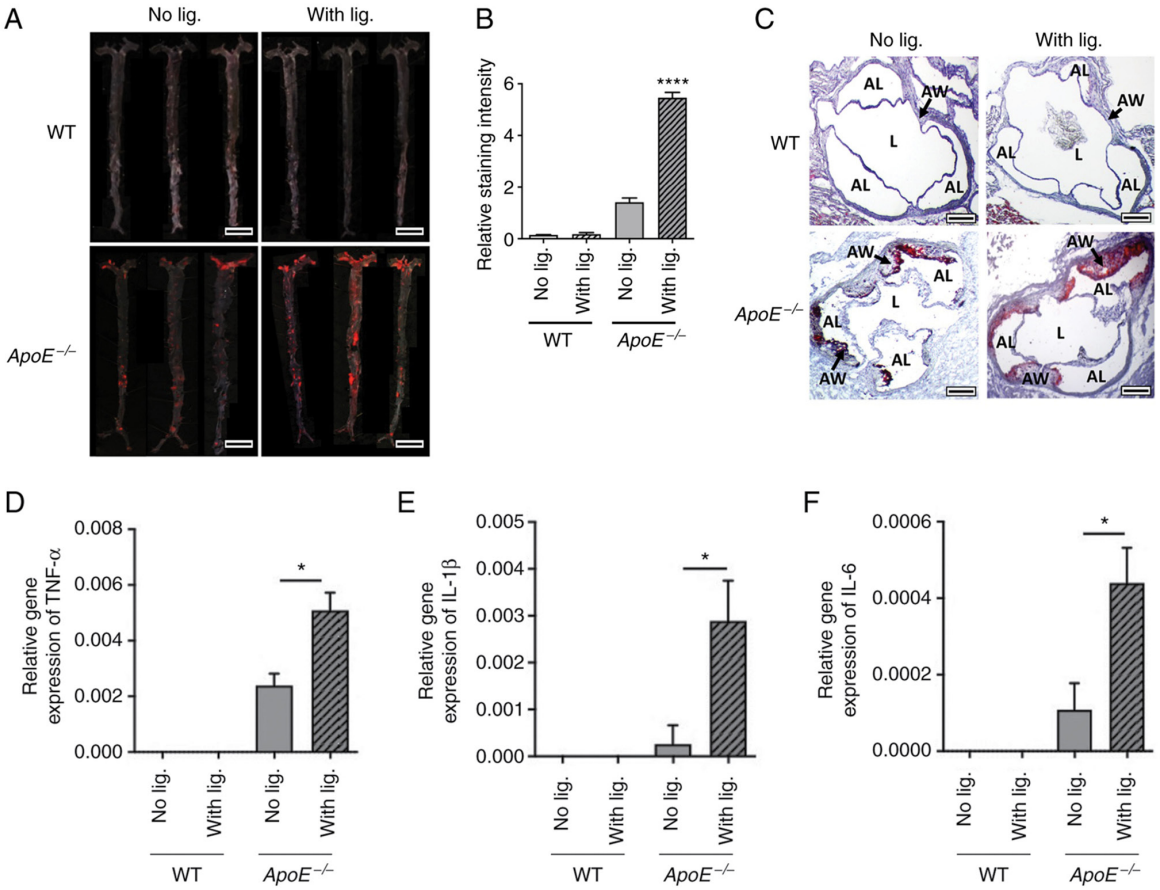

Figure 5. Development of vascular inflammation and atherosclerosis in WT and *ApoE*$^{-/-}$ mice fed with HFD. (A) Images of mice aortas from the *en face* preparation after staining with Sudan IV (scale bar, 5 mm). (B) Quantification of the *en face* analysis. The intensity of lipid staining was compared: Results represent the means ± SEM from 5 different samples. ****P<0.0001 vs. *ApoE*$^{-/-}$ with no ligation. (C) Representative examples of cross sections from Oil Red O-stained aortic root (scale bar, 200 μm). Gene expression levels of (D) TNF-α, (E) IL-1β and (F) IL-6 from aortic tissue determined using RT-qPCR. β-actin served as loading control. Results represent the means ± SEM from 5 different samples. *P<0.05. WT, wild-type; *ApoE*$^{-/-}$, Apolipoprotein E-deficient; HFD, high-fat diet; AL, aortic leaflet; AW, aortic wall; L, lumen.

en face analysis was performed to quantify the lipid deposition on the arterial wall. WT mice did not develop notable lipid depositions in both with or without ligature placement groups. By contrast, *ApoE*$^{-/-}$ mice revealed significantly increased lipid deposition in ligatured mice compared with the non-ligatured group (Fig. 5A and B). Similarly, the Oil Red-O staining of aortic roots also demonstrated increased deposition of lipid in the vessel walls of *ApoE*$^{-/-}$ mice receiving ligature placement compared with those in *ApoE*$^{-/-}$ mice without ligature placement, but no notable lipid deposition was observed in the WT mice regardless of ligature placement (Fig. 5C).

When gene expression levels of the pro-inflammatory cytokines were measured from the aorta using RT-qPCR, the present study revealed negligible levels in WT mice whether the ligature was placed or not (Fig. 5D-F). By contrast, there was a significant increase in the expression levels of TNF-α, IL-1β and IL-6 in the arterial wall in *ApoE*$^{-/-}$ mice with ligature placement compared with *ApoE*$^{-/-}$ mice without ligature placement (Fig. 5D-F). These data indicated that ligature-induced periodontitis increased vascular inflammation and aortic lipid deposition in *ApoE*$^{-/-}$ mice, but not in WT mice.

Discussion

In the present study, severe periodontitis was introduced in both WT and *ApoE*$^{-/-}$ mice by a long-term ligature placement around the second molars. WT mice did not develop atherosclerosis even under extreme conditions such as severe periodontitis and HFD Meanwhile, HFD alone moderately developed atherosclerosis in *ApoE*$^{-/-}$ mice, but the ligature-induced severe periodontal disease significantly exacerbated the development of atherosclerosis.

It is worth noting that WT mice seldomly develop atherosclerosis, which is attributed to their innate capacity to lowering lipid contents (25,26). In the present study, serum lipids in WT mice were significantly decreased compared with those in *ApoE*$^{-/-}$ mice when both groups were exposed to HFD. One of the major functions of ApoE protein is to serve as a ligand for the LDL receptor and to facilitate uptake and clearance of various lipoprotein complexes (27). Subsequently, the current study clearly demonstrated and verified that elevated lipid levels are a *bona fide* pre-requisite for atherosclerosis development.

Notably, severe periodontitis induced by the ligature placement did not alter the levels of lipids in WT mice when compared with WT mice without periodontitis, despite the significant increase of systemic inflammation by periodontitis. Previous clinical studies demonstrate rather conflicting results on the association between periodontitis and lipid levels; some studies have revealed a positive correlation while others demonstrated it to be insignificant (28-31). Based on the present data, it was hypothesized that ligature-induced periodontitis did not directly affect the lipid levels in serum and that ligature-induced periodontitis and lipid levels may be independent risk factors for the atherosclerosis development in mice.

The present study indicated that the levels of pro-inflammatory cytokines such as IL-1β, IL-6 and TNF-α were all significantly elevated in *ApoE*$^{-/-}$ mice in the presence of severe periodontitis, which suggested that these cytokines were putative therapeutic targets for the atherosclerosis. Indeed, the utilization of anti-IL-6 or anti-TNF-α therapy such as infliximab or tocilizumab have been suggested in clinics; however, however, their negative side effects decrease their likelihood of being used (32,33). By contrast, a previous clinical trial, Canakinumab Anti-inflammatory Thrombosis Outcomes Study, demonstrated that Canakinumab, an anti-IL-1β antibody, effectively reduces recurrent major adverse cardiovascular events (34). Overall, these clinical studies underscore the importance of systemic inflammation in mediating the development of atherosclerosis.

Although the present study demonstrated an association between severe periodontitis and the development of atherosclerosis in *ApoE*$^{-/-}$ mice, the molecular mechanism of this link remains unknown. However, there are several explanations for this association. First, severe periodontitis induces chronic inflammation, which results in persistent pro-inflammatory cytokines at the local level and releases them systemically throughout the body, such that it ultimately affects atherosclerosis in hyperlipidemic condition. Second, the oral bacteria responsible for periodontal disease might induce the development of atherosclerosis. Indeed, *Actinobacillus actinomycetemcomitans* and *Porphyromonas gingivalis* have been revealed in atherosclerotic lesions in humans (35). In addition, oral inoculation of *Porphyromonas gingivalis* induces atherosclerosis in experimental hyperlipidemic mouse models (36,37). However, given that other 'sterile' inflammatory conditions, such as SLE, are also a risk factor for atherosclerosis (38), the sole role of bacteria requires further clarification. Lastly, chronic and persistent periodontal disease may trigger alterations in local immunity (via epigenetics) such that it permanently changes the behaviors of the key players in atherosclerosis (39,40). The fundamental mechanisms of periodontitis-induced atherosclerosis development need to be further investigated.

There are several limitations to the present study. First, although *ApoE*$^{-/-}$ mice are well-established to represent studies on atherosclerosis, global knockout of *ApoE* in other cells make it challenging to rule out involvement of confounding cells (41,42). As such, it may require additional validation of the present findings with other mouse models such as *LDLR*$^{-/-}$ mice. Second, 14 weeks of ligature placement were used to mimic chronic periodontal disease conditions. However, it remains to be determined whether 14 weeks of ligature in mice truly represents chronic periodontal disease in humans. Third, involvement of the oral microbiome cannot be ruled out because, as aforementioned, several known oral bacterial species are found in the atherosclerotic lesions (35-37) and play a direct pathologic role in atherosclerosis development.

In summary, the present study suggested that severe periodontal diseases were a significant risk factor for exacerbating atherosclerosis under specific conditions, such as hyperlipidemia. In addition, periodontal disease and high cholesterol were seemingly independent risk factors for atherosclerosis development, and the coupling of systemic inflammation and hyperlipidemia may be necessary for the development and exacerbation of atherosclerosis induced by periodontitis. Alleviating chronic periodontal disease could potentially be a novel therapeutic method to intervene in atherosclerosis development in high-risk groups.

Acknowledgements

Not applicable.

Funding

This work was supported in part by the research funds awarded from the UCLA Chancellor's Office and National Institutes of

Health/National Institute of Dental and Craniofacial Research (grant no. R01DE 023348).

Availability of data and materials

The datasets used and/or analyzed during the current study are available from the corresponding author on reasonable request.

Authors' contributions

NHP and RK were involved in the conceptualization of the study. JS, SK, and SHL performed the experiments and participated in data analysis. JS, SK and SHL confirmed the authenticity of all the raw data. JS, SK, SHL, RK and NHP were involved in the discussion and interpretation of the results. JS, SK, RK, and NHP drafted the manuscript. All authors have read and approved the final manuscript.

Ethics approval and consent to participate

All procedures were performed in compliance with the institution's policy and applicable provisions of the United States Department of Agriculture (USDA) Animal Welfare Act Regulations and the Public Health Service (PHS) Policy. The experimental protocols were approved by the Animal Research Committee of the University of California, Los Angeles (approval no. ARC# 2019-057).

Patient consent for publication

Not applicable.

Competing interests

The authors declare that they have no competing interests.

References

1. Eke PI, Dye BA, Wei L, Thornton-Evans GO and Genco RJ; CDC Periodontal Disease Surveillance workgroup: James Beck (University of North Carolina, Chapel Hill, USA), Gordon Douglass (Past President, American Academy of Periodontology), Roy Page (University of Washin: Prevalence of periodontitis in adults in the United States: 2009 and 2010. J Dent Res 91: 914-920, 2012.
2. Eke PI, Dye BA, Wei L, Slade GD, Thornton-Evans GO, Borgnakke WS, Taylor GW, Page RC, Beck JD and Genco RJ: Update on prevalence of periodontitis in adults in the United States: NHANES 2009 to 2012. J Periodontol 86: 611-622, 2015.
3. Dzink JL, Tanner AC, Haffajee AD and Socransky SS: Gram negative species associated with active destructive periodontal lesions. J Clin Periodontol 12: 648-659, 1985.
4. Kinane DF, Zhang P, Benakanakere M, Singleton J, Biesbrock A, Nonnenmacher C and He T: Experimental gingivitis, bacteremia and systemic biomarkers: A randomized clinical trial. J Periodontal Res 50: 864-869, 2015.
5. Slots J: Periodontitis: Facts, fallacies and the future. Periodontol 75: 7-23, 2000.
6. Rydén L, Buhlin K, Ekstrand E, de Faire U, Gustafsson A, Holmer J, Kjellström B, Lindahl B, Norhammar A, Nygren Å, *et al*: Periodontitis increases the risk of a first myocardial infarction: A report from the PAROKRANK study. Circulation 133: 576-583, 2016.
7. Slocum C, Kramer C and Genco CA: Immune dysregulation mediated by the oral microbiome: Potential link to chronic inflammation and atherosclerosis. J Intern Med 280: 114-128, 2016.
8. Jain A, Batista EL Jr, Serhan C, Stahl GL and Van Dyke TE: Role for periodontitis in the progression of lipid deposition in an animal model. Infect Immun 71: 6012-6018, 2003.
9. Hasturk H, Abdallah R, Kantarci A, Nguyen D, Giordano N, Hamilton J and Van Dyke TE: Resolvin E1 (RvE1) attenuates atherosclerotic plaque formation in diet and inflammation-induced atherogenesis. Arterioscler Thromb Vasc Biol 35: 1123-1133, 2015.
10. Joshi NV, Toor I, Shah AS, Carruthers K, Vesey AT, Alam SR, Sills A, Hoo TY, Melville AJ, Langlands SP, *et al*: Systemic atherosclerotic inflammation following acute myocardial infarction: Myocardial infarction begets myocardial infarction. J Am Heart Assoc 4: e001956, 2015.
11. Soehnlein O and Libby P: Targeting inflammation in atherosclerosis-from experimental insights to the clinic. Nat Rev Drug Discov 20: 589-610, 2021.
12. Hansson BG, Rosenquist K, Antonsson A, Wennerberg J, Schildt EB, Bladström A and Andersson G: Strong association between infection with human papillomavirus and oral and oropharyngeal squamous cell carcinoma: A population-based case-control study in southern Sweden. Acta Otolaryngol 125: 1337-1344, 2005.
13. Libby P, Ridker PM and Hansson GK: Progress and challenges in translating the biology of atherosclerosis. Nature 473: 317-325, 2011.
14. Gargiulo P, Marsico F, Parente A, Paolillo S, Cecere M, Casaretti L, Pellegrino AM, Formisano T, Fabiani I, Soricelli A, *et al*: Ischemic heart disease in systemic inflammatory diseases. An appraisal. Int J Cardiol 170: 286-290, 2014.
15. Offenbacher S, Beck JD, Moss K, Mendoza L, Paquette DW, Barrow DA, Couper DJ, Stewart DD, Falkner KL, Graham SP, *et al*: Results from the Periodontitis and Vascular Events (PAVE) Study: A pilot multicentered, randomized, controlled trial to study effects of periodontal therapy in a secondary prevention model of cardiovascular disease. J Periodontol 80: 190-201, 2009.
16. Beck J, Garcia R, Heiss G, Vokonas PS and Offenbacher S: Periodontal disease and cardiovascular disease. J Periodontol 67 (Suppl 10): S1123-S1137, 1996.
17. Suh JS, Kim S, Boström KI, Wang CY, Kim RH and Park NH: Periodontitis-induced systemic inflammation exacerbates atherosclerosis partly via endothelial-mesenchymal transition in mice. Int J Oral Sci 11: 21, 2019.
18. Oberoi R, Vlacil AK, Schuett J, Schösser F, Schuett H, Tietge UJF, Schieffer B and Grote K: Anti-tumor necrosis factor-α therapy increases plaque burden in a mouse model of experimental atherosclerosis. Atherosclerosis 277: 80-89, 2018.
19. Suh JS, Lee SH, Fouladian Z, Lee JY, Kim T, Kang MK, Lusis AJ, Boström KI, Kim RH and Park NH: Rosuvastatin prevents the exacerbation of atherosclerosis in ligature-induced periodontal disease mouse model. Sci Rep 10: 6383, 2020.
20. Kim T, Kim S, Song M, Lee C, Yagita H, Williams DW, Sung EC, Hong C, Shin KH, Kang MK, *et al*: Removal of pre-existing periodontal inflammatory condition before tooth extraction ameliorates medication-related osteonecrosis of the jaw-like lesion in mice. Am J Pathol 188: 2318-2327, 2018.
21. Huang Q, Qin L, Dai S, Zhang H, Pasula S, Zhou H, Chen H and Min W: AIP1 suppresses atherosclerosis by limiting hyperlipidemia-induced inflammation and vascular endothelial dysfunction. Arterioscler Thromb Vasc Biol 33: 795-804, 2013.
22. Livak KJ and Schmittgen TD: Analysis of relative gene expression data using real-time quantitative PCR and the 2(-Delta Delta C (T)) method. Methods 25: 402-408, 2001.
23. Lamont RJ, Koo H and Hajishengallis G: The oral microbiota: Dynamic communities and host interactions. Nat Rev Microbiol 16: 745-759, 2018.
24. Mussbacher M, Salzmann M, Brostjan C, Hoesel B, Schoergenhofer C, Datler H, Hohensinner P, Basílio J, Petzelbauer P, Assinger A and Schmid JA: Cell type-specific roles of NF-κB linking inflammation and thrombosis. Front Immunol 10: 85, 2019.
25. Getz GS and Reardon CA: Animal models of atherosclerosis. Arterioscler Thromb Vasc Biol 32: 1104-1115, 2012.
26. Pendse AA, Arbones-Mainar JM, Johnson LA, Altenburg MK and Maeda N: Apolipoprotein E knock-out and knock-in mice: Atherosclerosis, metabolic syndrome, and beyond. J Lipid Res 50 (Suppl): S178-S182, 2009.
27. Mahley RW: Apolipoprotein E: Cholesterol transport protein with expanding role in cell biology. Science 240: 622-630, 1988.

28. Machado AC, Quirino MR and Nascimento LF: Relation between chronic periodontal disease and plasmatic levels of triglycerides, total cholesterol and fractions. Braz Oral Res 19: 284-289, 2005.
29. Valentaviciene G, Paipaliene P, Nedzelskiene I, Zilinskas J and Anuseviciene OV: The relationship between blood serum lipids and periodontal condition. Stomatologija 8: 96-100, 2006.
30. Thapa S and Wei F: Association between high serum total cholesterol and periodontitis: National Health and nutrition examination survey 2011 to 2012 study of American adults. J Periodontol 87: 1286-1294, 2016.
31. Lee S, Im A, Burm E and Ha M: Association between periodontitis and blood lipid levels in a Korean population. J Periodontol 89: 28-35, 2018.
32. IL6R Genetics Consortium Emerging Risk Factors Collaboration, Sarwar N, Butterworth AS, Freitag DF, Gregson J, Willeit P, Gorman DN, Gao P, Saleheen D, Rendon A, *et al*: Interleukin-6 receptor pathways in coronary heart disease: A collaborative meta-analysis of 82 studies. Lancet 379: 1205-1213, 2012.
33. Mann DL: Innate immunity and the failing heart: The cytokine hypothesis revisited. Circ Res 116: 1254-1268, 2015.
34. Ridker PM, Everett BM, Thuren T, MacFadyen JG, Chang WH, Ballantyne C, Fonseca F, Nicolau J, Koenig W, Anker SD, *et al*: Antiinflammatory therapy with canakinumab for atherosclerotic disease. N Engl J Med 377: 1119-1131, 2017.
35. Kozarov EV, Dorn BR, Shelburne CE, Dunn WA Jr and Progulske-Fox A: Human atherosclerotic plaque contains viable invasive Actinobacillus actinomycetemcomitans and Porphyromonas gingivalis. Arterioscler Thromb Vasc Biol 25: e17-e18, 2005.
36. Gibson FC III, Hong C, Chou HH, Yumoto H, Chen J, Lien E, Wong J and Genco CA: Innate immune recognition of invasive bacteria accelerates atherosclerosis in apolipoprotein E-deficient mice. Circulation 109: 2801-2806, 2004.
37. Lalla E, Lamster IB, Hofmann MA, Bucciarelli L, Jerud AP, Tucker S, Lu Y, Papapanou PN and Schmidt AM: Oral infection with a periodontal pathogen accelerates early atherosclerosis in apolipoprotein E-null mice. Arterioscler Thromb Vasc Biol 23: 1405-1411, 2003.
38. Wigren M, Nilsson J and Kaplan MJ: Pathogenic immunity in systemic lupus erythematosus and atherosclerosis: Common mechanisms and possible targets for intervention. J Intern Med 278: 494-506, 2015.
39. Xu S, Pelisek J and Jin ZG: Atherosclerosis is an epigenetic disease. Trends Endocrinol Metab 29: 739-742, 2018.
40. Koelwyn GJ, Corr EM, Erbay E and Moore KJ: Regulation of macrophage immunometabolism in atherosclerosis. Nat Immunol 19: 526-537, 2018.
41. Daugherty A, Tall AR, Daemen MJAP, Falk E, Fisher EA, García-Cardeña G, Lusis AJ, Owens AP III, Rosenfeld ME and Virmani R, *et al*: Recommendation on design, execution, and reporting of animal atherosclerosis studies: A scientific statement from the american heart association. Circ Res 121: e53-e79, 2017.
42. Hinder LM, Vincent AM, Hayes JM, McLean LL and Feldman EL: Apolipoprotein E knockout as the basis for mouse models of dyslipidemia-induced neuropathy. Exp Neurol 239: 102-110, 2013.